Quantum Dielectric Theory of Electronegativity in Covalent Systems. II. Ionization Potentials and Interband Transition Energies

J. A. VAN VECHTEN*
Bell Telephone Laboratories, Murray Hill, New Jersey 07974
(Received 21 April 1969)

We construct a dielectric two-band model which describes and predicts ionization potentials and electronic band structures of binary compounds A_NB_{8-N}. Only the density and dielectrically defined electronegativity difference are required as input data. The method is applied to 19 tetrahedrally coordinated crystals with excellent results. Predictions are also made for 18 other tetrahedrally coordinated crystals. The extension to octahedral coordination is discussed, and direct band gaps are calculated for 28 such crystals. It is also proposed that crystal structure and phase transitions can be predicted using this method.

I. INTRODUCTION

IN the first paper of this series,[1] we developed the concept of electronegativity difference as a scaling parameter which generalizes the concepts of valence and size differences. To treat the low-frequency electronic polarizabilities of diatomic crystals with formula A_NB_{8-N}, we introduced a simple quantum-mechanical model to describe s-p valence bond susceptibilities.[2] An average energy gap E_g is deduced from the real, static, electronic dielectric constant $\epsilon_1(0)$. In tetrahedrally coordinated crystals, E_g represents the energy difference between bonding and antibonding (sp^3) hybridized orbitals. It may be decomposed into contributions due to the symmetric and the antisymmetric parts of the potential within the unit cell.[1,3] We denote these contributions by E_h and C, respectively. The decomposition of E_g is

$$E_g^2=E_h^2+C^2. \tag{1.1}$$

Because $C=0$ by symmetry for a homopolar (diamond-type) crystal, $E_h=E_g$ is fixed for the group-IV elements by observation of $\epsilon_1(0)$. In I we showed that E_h is a function of nearest-neighbor distance only. Thus E_h is fixed for the diatomic crystal formed from elements α and β by interpolation based on the nearest-neighbor distance. $C_{\alpha\beta}$ is determined from the electronic dielectric constant $\epsilon_1(0)$. (It has been found that the nearest-neighbor distance in all diamond, zincblende, and wurtzite crystals formed of elements from a given pair of rows of the Periodic Table is nearly constant, so that E_h is nearly constant for all such crystals. This effect was utilized by Cohen and Bergstresser[4] in their band-structure calculations.)

When α and β belong to the same row of the Periodic Table, $C_{\alpha\beta}$ is found to be proportional to the valence difference $\Delta Z=|Z_\alpha-Z_\beta|$. Therefore, we regard the empirically determined values of $C_{\alpha\beta}$ as a generalization of the concept of valence difference to include the effects of row or ion core differences when α and β belong to different rows. In this sense we take the value of $C_{\alpha\beta}$ to be a dielectric definition of the electronegativity difference between elements α and β.

In I, relatively simple expressions are used for $\epsilon_1{}^{\alpha\beta}(0)$ and $C_{\alpha\beta}$. For $\epsilon_1(0)$ we have

$$\epsilon_1{}^{\alpha\beta}(0)=1+(\hbar\omega_p)^2DA/(Eh^2+C_{\alpha\beta}{}^2), \tag{1.2}$$

where

$$A=1-B+\tfrac{1}{3}B^2, \tag{1.3}$$

$$B=E_g/4E_F, \tag{1.4}$$

and where E_F and ω_p are the free-electron Fermi energy and plasma frequency calculated for a density of eight electrons per unit cell (or four per atomic volume) and D is the square of the ratio of the effective plasma frequency to this free-electron value. (As is explained in I, the presence of a filled d-electron band below the valence band in crystals containing elements from the third and fourth rows introduces into the f sum negative terms because of the interaction of the d band with the valence band. Thus the sum of the oscillator strengths connecting the valence and conduction bands is greater than four and the effective plasma frequency is greater than the free-electron value.[5]) The factor D is discussed at length in I, and a prescription for its evaluation when an experimental determination is lacking is given by Eq. (3.11) of I. We do not repeat that discussion here but include the values obtained in Table V. For C we have

$$C=b\left(\frac{Z_\alpha}{r_\alpha}-\frac{Z_\beta}{r_\beta}\right)\exp\left(-k_s\frac{r_\alpha+r_\beta}{2}\right), \tag{1.5}$$

where k_s is the linearized Thomas-Fermi screening wave number, and $r_{\alpha,\beta}$ is the covalent radius of element α,β. We have defined the covalent radius as half the nearest-neighbor distance in the diamond-type crystal of the group-IV element in the row to which element α,β belongs times the ratio of the observed lattice

* Fannie and John Hertz Foundation Fellow.
[1] J. A. Van Vechten, Phys. Rev. **182**, 891 (1969), hereafter referred to as I.
[2] D. Penn, Phys. Rev. **128**, 2093 (1962).
[3] J. C. Phillips, Phys. Rev. Letters **20**, 550 (1968).
[4] M. L. Cohen and T. K. Bergstresser, Phys. Rev. **141**, 789 (1966).
[5] This is discussed by H. R. Philipp and H. Ehrenreich, Phys. Rev. **129**, 1550 (1962), who show some empirical observation of this effect. See also F. Seitz, *Modern Theory of Solids* (McGraw-Hill Book Co., New York, 1940), p. 644.

constant of the crystal to the "normal covalent" value, which is the geometric mean of the lattice constants of those diamond-type crystals corresponding to α and β. (As noted above, this ratio is nearly unity for all zinc-blende and wurtzite crystals.) The prefactor b is found empirically to have the constant value 1.5 within 7% for tetrahedrally coordinated crystals; its dependence on density in ionic, octahedrally coordinated crystals is discussed in I.

In this paper we wish to extend the analysis of I to treat (1) ionization energies from the top of the valence band to vacuum, and (2) transition energies associated with specific edges in the imaginary part of the dielectric constant $\epsilon_2(\omega)$. In principle, $\epsilon_1(0)$ may be determined from $\epsilon_2(\omega)$ by the Kramers-Kronig relation

$$\epsilon_1(0)=1+\frac{2}{\pi}\int_0^\infty \frac{\epsilon_2(\omega)}{\omega}d\omega. \tag{1.6}$$

Thus the dependence of $\epsilon_1(0)$ on E_h and C is actually a composite of the energy dependence of all the interband gaps. (It may also be affected by some redistribution of oscillator strength between various transitions.) We have already noted in I that E_g is approximately the energy of the largest peak in $\epsilon_2(\omega)$, both for homopolar and heteropolar crystals.

Because the present analysis enables us to predict interband energies associated with specific energy levels, $E_n(\mathbf{k}_\alpha)$, at definite points $\mathbf{k}_\alpha$ in the Brillouin zone, it is in some respects an empirical energy band calculation. One might regard each interband edge and the value of that energy gap in the appropriate homopolar crystal as together defining an effective value of $C_{\alpha\beta}$ the average ionic potential. To the extent that different edges involve similarly weighted averages, the one set of values of C that we have determined in I from $\epsilon_1(0)$ together with the observed band structures in the diamond-type crystals serve to predict all the other band structures. Thus, in contrast to the empirical pseudopotential method, this approach avoids the task of constructing and Fourier-analyzing a one-electron crystal potential as well as solving the large secular equations derived from the Schrödinger equation.

Before proceeding, an historical remark is in order. The idea of separating the effects of covalency and ionicity and treating the latter as a perturbation in order to predict the energy differences in zinc-blende crystals from those in diamond-type crystals was first put forward some time ago by Herman.[6] He observed that for a horizontal sequence of crystals (e.g., Ge, GaAs, ZnSe), the fundamental gap increases as the square of the valence difference ΔZ. (Herman calls this parameter λ and graphs showing this relationship are widely known as λ^2 plots.) Herman's analysis has been extended to other energy gaps as well. A simple perturbation interpretation, analogous to our treatment of E_g, would predict that a given gap E_i should increase as

$$E_i=E_{i,h}(1+\kappa_i^2\Delta Z^2/E_{i,h}^2)^{1/2}, \tag{1.7}$$

where $E_{i,h}$ is the value of E_i for the appropriate homopolar crystal and κ_i is some constant. However, empirically some energy gaps increase as found by Herman for E_0, i.e., as

$$E_i=E_{i,h}+\kappa_i^2\Delta Z^2/2E_{i,h}. \tag{1.8}$$

Thus for some gaps λ^2 plots turn over into the curve indicated by (1.7), while for others the plot remains an approximately straight line.

The present model can be regarded as an extension of Herman's work to describe skew crystals, such as InP and AlSb, that do not fit into his horizontal sequences, by generalizing from λ or ΔZ to C. We note that Eq. (1.1) requires only that the average gap E_g follow the form of Eq. (1.7):

$$E_g=E_{g,h}(1+C^2/E_{g,h}^2)^{1/2}. \tag{1.7'}$$

Also, in our two-band model (1.7') corresponds to an exact solution of the 2×2 Hamiltonian and not to a second-order perturbation. Thus our analysis may be applied to cases where $C>E_h$ as occur in II-VI compounds. An explanation of the approximately linear dependence of several of the E_i's is given on the basis of the effect of the filled d band in many of the crystals. In doing this we will utilize some of the wealth of new data which has become available on the fundamental absorption spectra over a wide energy range[7] as well as the interpretation of those data through extensive pseudopotential calculations.[4,8]

Although the photoemission and work-function data are by no means as complete as the optical data, we will consider first, in Sec. II, the absolute energy, i.e., relative to the vacuum state, of the state labeled $\Gamma_{25'}$ or $\Gamma_{15,v}$ (at the top of the valence band) and the dependence of this on our electronegativity parameter C. This will allow us to establish the absolute energy of the states at the other critical points within the bands from a knowledge of the direct and indirect gaps. In Sec. III, we propose an extremely simple method for calculating the band structures of tetrahedrally coordinated crystals. We then compare the result of our calculation with the experimental interband energy gaps of 19 diamond, zinc-blende, and wurtzite crystals and also with the results of the empirical pseudopotential method. In Sec. V we consider the relation among our parameters, E_h and C, the band structure, and the crystal type in which the compound is found. In Sec. VI we discuss the extension of our results to the rocksalt structure. A discussion of the pressure dependence of the energy gaps will be published separately.[9]

[6] F. Herman, J. Electron. 1, 103 (1955).

[7] J. C. Phillips, in *Solid State Physics*, edited by F. Seitz and D. Turnbull (Academic Press Inc., New York, 1966), Vol. 18.

[8] D. Brust, Phys. Rev. 134, A1337 (1964).

[9] J. C. Phillips and J. A. Van Vechten (unpublished).

TABLE I. Nomenclature of interband energy gaps commonly used in the literature. Note that the designation of points in the Brillouin zone is meant to indicate the symmetry of the transitions; the actual energy gap at the points indicated is not always the energy of the corresponding critical point in the spectrum or the joint density of states. For instance, in diamond it is known that the lowest indirect gap is from Γ to a point on the Δ axis 77% of the way from Γ to X (see Ref. 20).

Label	Transition				
	Diamond	Zinc-blende	Wurtzite	NaCl	Symmetry
I	$\Gamma_{25}' \rightarrow Vac$	$\Gamma_{15,v} \rightarrow Vac$	$\Gamma_{1,v},\Gamma_{6,v} \rightarrow Vac$	$\Gamma_{15} \rightarrow Vac$	$P \rightarrow$
E_0	$\Gamma_{25}' \rightarrow \Gamma_2'$	$\Gamma_{15,v} \rightarrow \Gamma_{1,c}$	$\Gamma_{1,v},\Gamma_{6,v} \rightarrow \Gamma_{1,c}$	$\Gamma_{15} \rightarrow \Gamma_1$	$P \rightarrow S$
E_1	$L_3' \rightarrow L_1$	$L_{3,v} \rightarrow L_{1,c}$	$\Gamma_{5,v} \rightarrow \Gamma_{3,c}$	$L_3 \rightarrow L_2'$	$P \rightarrow S$
E_{2A}	$X_4 \rightarrow X_1$	$X_5 \rightarrow X_1$	$K_{3,v} \rightarrow K_{2,c}$	$X_5' \rightarrow X_3$	
			$H_{3,v} \rightarrow H_{3c}$		$P \rightarrow \frac{1}{2}S$
E_{2B}	$X_4 \rightarrow X_1$	$X_5 \rightarrow X_3$	$K_{2,v} \rightarrow K_2$	$X_5' \rightarrow X_1$	
E_0'	$L_{25}' \rightarrow \Gamma_{15}$	$\Gamma_{15,v} \rightarrow \Gamma_{15,c}$	$\Gamma_{1,v},\Gamma_{6,v} \rightarrow \Gamma_{1,c},\Gamma_{6,c}$	$\Gamma_{15} \rightarrow \Gamma_{25}'$	$P \rightarrow P$
E_1'	$L_3' \rightarrow L_3$	$L_{3,v} \rightarrow L_{3,c}$	$\Gamma_{5,v} \rightarrow \Gamma_{6,c}$	$L_3 \rightarrow L_3'$	$P \rightarrow P$
$E_{\text{ind } X}$	$\Gamma_{25}' \rightarrow X_1$	$\Gamma_{15,v} \rightarrow X_1$	$\Gamma_{6,v} \rightarrow H_3$	$\Gamma_{15} \rightarrow X_3$	$P \rightarrow \frac{1}{2}S$
			K_2		
$E_{\text{ind } L}$	$\Gamma_{25}' \rightarrow L_1$	$\Gamma_{15,v} \rightarrow L_{1,c}$	$\Gamma_{6,v} \rightarrow U_3$	$\Gamma_{15} \rightarrow L_2'$	$P \rightarrow S$

We present in Table I a synopsis of the energy-gap nomenclature in common use in the literature. Table II summarizes all the parameters deduced or used. Our results are presented in Tables III, VI, and VII.

II. IONIZATION POTENTIALS

As noted above, we found in I that the average homopolar energy gap $E_{g,h}$ was a function of nearest-neighbor distance only. Here we will assume that the homopolar energy of all wave functions, except those of s-like symmetry which are affected by the presence of a filled d band, is a function of nearest-neighbor distance only.

Consider the p-like state $\Gamma_{25'}$ which has the maximum energy of the valence band in all group-IV crystals. Allen and Gobeli[10] measured the energy of this state relative to the vacuum level in Si and Ge by careful extrapolation of very low photoemissive yields. Their values for the position of the $J=\frac{3}{2}$ $\Gamma_{25'}$ level relative to vacuum are -5.15 and -4.80 eV, respectively. When we remove the effect of spin-orbit splitting we obtain -5.17 and -4.90 eV, respectively, for the center of gravity of the $\Gamma_{25'}$ level. (The effect of spin-orbit splitting will be removed from all data quoted hereafter.) Thus the logarithmic derivative of the ionization potential $E_{\text{vac}}-E_{\Gamma_{25'}}\equiv I$, with respect to nearest-neighbor distance d, is -1.31, and assuming $I \propto d^s$ with $s=-1.31$, we may calculate the value of I for a homopolar crystal of any given d. We denote this quantity as I_h.

With these values of I_h and the value of C that we found in I, we may calculate I for other crystals using

$$I=I_h[1+(C/I_h)^2]^{1/2}. \quad (2.1)$$

These values have been included in Table III, where they may be compared to the experimental values which have been determined for 12 III–V and II–VI crystals.[11–14] We note that all 12 predictions agree with experiment to within 10% and eight of the 12 to within 3%. For the higher values of I reliable experimental values are obtained only from crystals cleaved in high vacuum.

We believe that this level of discrepancy is not greater than is to be expected from the combined effects of experimental error, error in the determination of C in I, and the inaccuracy in extrapolating I_h from the experimental values for Si and Ge, which differ in d by only about 4%. (See Fig. 1.) The experiment is complicated by the requirements that the sample surface be atomically clean and that the quantum yield be pursued to about 10^{-5} electrons/absorbed photon to obtain the threshold. Shay and Spicer[15] showed that the difference in sample surface between crystals cleaved and measured in a 10^{-4}- and in a 10^{-9}-Torr

TABLE II. Parameters used in the calculations presented. Al factors except Vac-X_4 [see Eqs. (2.1), (3.1), (3.3), and (3.7)] are obtained by extrapolating the value assumed for Si as a function of observed nearest-neighbor distance using only the logarithmic derivatives listed. Vac-X_4 is evaluated using the normal covalent nearest-neighbor distance instead of the observed value. $(X_3-X_1)/C=0.071$ gives the splitting of the X_3 and X_1 conduction states as a function of electronegativity difference (3.6).

Parameter	Value for Si	Log. deriv.
I_h	5.17	-1.3077
Vac-X_4	8.63	-1.43
E_{0h}	4.10	-2.75
E_{1h}	3.60	-2.22
E_{2h}	4.50	-2.3821
E_{0h}'	3.40	-1.92
E_1'	5.90	-1.67
ΔE_0	12.80	-5.07
ΔE_1	4.976	-4.97

[10] F. G. Allen and G. W. Gobeli, Phys. Rev. **144**, 558 (1966).

[11] T. E. Fischer, Phys. Rev. **139**, A1228 (1965).
[12] T. E. Fischer, Phys. Rev. **142**, 519 (1966).
[13] M. C. Cohen and J. C. Phillips, Phys. Rev. **139**, A912 (1965).
[14] R. K. Swank, Phys. Rev. **153**, 844 (1967).
[15] J. L. Shay and W. E. Spicer, Phys. Rev. **161**, 799 (1967); **169**, 650 (1968); **175**, 741 (1968).

vacuum may result in a shift in the apparent threshold of more than 1 eV. Swank's results[14] indicate that in some cases a 10^{-11}-Torr vacuum is required. While surface contamination tends to lower the apparent threshold, not pursuing the quantum yield to a low enough level tends to overestimate the value. This is because the quantum yield falls very sharply to about 10^{-4} electrons/quantum,[11,15] and then turns towards lower energy and follows a power law to the actual threshold.[16]

Once the value of I has been established, we may determine the absolute energy of the other states in the band structure and investigate their dependence on C and on d.

III. BAND STRUCTURES OF TETRAHEDRALLY COORDINATED CRYSTALS

In this paper we calculate band structures for tetrahedrally coordinated crystals under the following assumptions, which characterize the dielectric two-band model. The nature of the model is discussed at greater length in Sec. IV.

(1) In the absence of a filled d shell in one of the constituent atoms, all direct interband transition energies $E_{g,i}$ are given by the analog of Eq. (2.1), i.e., by

$$E_{g,i}=E_{h,i}(1+C^2/E_{h,i}^2)^{1/2} \tag{3.1}$$

if there is no filled d band.

(2) All the homopolar transition energies $E_{h,i}$ are a function of nearest-neighbor distance only and are determined by extrapolation from the values assumed in Si (see Table II). Thus

$$E_{h,i}(d)=(E_{h,i})_{\mathrm{Si}}(d/d_{\mathrm{Si}})^{s_i}. \tag{3.2}$$

(3) In all cases the absolute value of the $\Gamma_{25'}$ ($\Gamma_{15}{}^{v}$) level, the top of the valence band at the zone center, is determined by Eq. (2.1).

TABLE III. Comparison of theory and experiment for 19 tetrahedrally coordinated crystals for which relatively complete experimental data are available. Shown are the values omitting spin-orbit splitting obtained by empirical pseudopotential method according to Cohen, Bergstresser, and Saslow (see Refs. 4, 19, and 20), the experimental values, and the values as calculated in this paper (dielectric method). Whenever possible the experimental value was taken to be the peak of the electroreflectance structure or of the $\epsilon_2(\omega)$ spectrum at low temperature. When such data were not available, room-temperature data and reflectivity spectra were used. In the last column we show the results of an E_1' calculation assuming that this transition is 20% more sensitive to electronegativity difference than are the others. (See end of Sec. III.)

		Indirect gaps			Direct gaps						E_1' dielect prediction.
Crystal		I	Γ to X	Γ to L	E_0	E_1	E_{2A}	E_{2B}	E_0'	E_1'	corr.
	Pseudopot.		5.4	7.5	12.5	10.9	12.9	12.9	7.3	12.8	
C	Expt.		5.48[a]				12.2[b]	12.2[b]	7.3[b]		
	Dielect.	8.96	5.48	5.77	13.04	9.16	12.26	12.26	7.63	11.91	11.91
	Pseudopot.										
BP	Expt.		2.0[c]			5[d]	6.9[d]			8.0[d]	8.0[d]
	Dielect.	6.58	1.81	2.88	6.76	5.42	6.89	7.00	4.86	8.00	8.02
	Pseudopot.										
SiC	Expt.		2.3–4.6[e]		7.75[f]	7.1[f]	8.3[f]		6.0[f]	9.7[f]	9.7[f]
	Dielect.	7.91	4.54	5.17	8.48	7.04	8.28	8.83	6.48	9.38	9.72
	Pseudopot.		0.8	1.9	3.8	3.1	4.0	4.0	3.4	5.2	
Si	Expt.	5.17[g]	1.13[h]		4.08[i]	3.6[j]	4.40[i]	4.40[i]	3.35[i]	5.4[g]	5.4[g]
	Dielect.	5.17	1.04	1.87	4.10	3.60	4.50	4.50	3.40	5.90	5.90
	Pseudopot.		2.2	2.7	2.7	3.6	4.6	4.9	5.3	6.4	
GaP	Expt.		2.38[k]		2.77[i]	3.73[i]	5.27[i]	5.74[i]	4.80[i]	6.6[l]	6.6[l]
	Dielect.	6.11	3.05	2.75	2.85	3.89	5.32	5.78	4.72	6.73	7.08
	Pseudopot.		5.2	5.3	3.7	5.8	6.7	7.5	8.9	9.2	
ZnS	Expt.	8.73±0.3[m]			3.80[n]	5.70[o]	7.6[n]	8.75[n]	6.65[n]	9.45[o]	9.45[o]
	Dielect.	8.09	6.96	5.72	4.37	5.87	7.25	8.13	7.08	8.59	9.52
	Pseudopot.		1.0	0.9	1.2	2.0	3.8	3.8	3.5	5.4	
Ge	Expt.	4.90[g]	0.96[h]	0.76[h]	0.89[i]	2.26[i]	4.3[p]	4.3[p]	3.19[i]	5.4[p]	5.4[p]
	Dielect.	4.90	0.84	0.61	0.96	2.23	4.08	4.08	3.14	5.51	5.51
	Pseudopot.		2.0	2.0	1.9	2.8	3.9	4.3	4.1	5.3	
AlSb	Expt.	5.47[q]	1.87[q]		2.5[i]	3.00[i]	4.25[i]	4.6[i]	3.81[i]	5.08[q]	5.08[q]
	Dielect.	5.39	2.15	2.39	2.67	3.49	4.36	4.80	4.11	5.73	6.08
	Pseudopot.		1.8	1.7	1.4	2.6	4.0	4.3	4.5	6.0	
GaAs	Expt.	5.59[r]	1.92[l]	2.0[l]	1.55[i]	3.04[i]	4.99[i]	5.33[i]	4.2[s]	6.2[l]	6.2[l]
	Dielect.	5.70	2.37	1.89	1.55	3.11	4.81	5.22	4.28	6.23	6.52
	Pseudopot.		2.3	2.0	1.6	2.8	4.2	4.5	4.6	6.0	
InP	Expt.	5.72[t]			1.37[i]	3.24[i]	4.8[p]	5.1[p]	4.4[p]	6.6[p]	6.6[p]
	Dielect.	5.74	2.93	2.25	1.45	3.17	4.78	5.25	4.44	6.17	6.55
	Pseudopot.		4.5	4.5	2.9	5.0	6.0	6.9	7.9	8.4	
ZnSe	Expt.	7.55[m]				4.95[o]	6.4[o]	7.2[o]		8.45[o]	8.45[o]
	Dielect.	7.43	5.82	4.26	3.37	5.09	6.52	7.32	6.42	7.85	8.68
	Pseudopot.				2.2	5.0	6.7	7.8	8.4	8.5	
CdS	Expt.	7.35[m]			2.48[n]	5.3[o]		7.8[u]	6.4[o]	8.8[o]	8.8[o]

[16] E. O. Kane, Phys. Rev. 127, 131 (1962).

TABLE III (*continued*)

Crystal		Indirect gaps I	Γ to X	Γ ro L	Direct gaps E_0	E_1	E_{2A}	E_{2B}	E_0'	E_1'	E_1' dielect. prediction corr.
	Dielect.	7.54	6.53	5.91	2.73	4.94	6.59	7.42	6.60	7.88	8.79
	Pseudopot.		2.1	1.6	0.8	2.3	3.8	4.2	4.4	5.6	
GaSb	Expt.	5.03[r]	1.30[l]	1.07[l]	0.99[l]	2.26[i]	4.1[o]	4.5[p]	3.37[i]	5.50[i]	5.50[i]
	Dielect.	4.90	1.36	1.17	1.00	2.41	3.84	4.14	3.43	5.27	5.45
	Pseudopot.		2.1	1.6	0.5	2.3	3.9	4.3	4.6	5.7	
InAs	Expt.	5.44[r]			0.5[p]	2.64[i]	4.5[p]	5.0[p]	3.7[s]	6.1[p]	6.1[p]
	Dielect.	5.27	2.14	1.45	0.56	2.41	4.25	4.64	3.90	5.65	5.94
	Pseudopot.		4.0	3.8	2.5	4.3	5.2	5.8	6.7	6.6	
ZnTe	Expt.	5.89[m]			2.56[i]	3.97[i]	5.3[p]		5.40[i]	7.20[o]	7.20[o]
	Dielect.	6.31	4.26	3.64	2.72	4.17	5.32	5.96	5.24	6.62	7.25
	Pseudopot.				2.0	4.3	6.0	7.2	7.7	7.9	
CdSe	Expt.	6.88[e]			1.87[i]	4.5[u]		6.9[u]	6[u]	8.35[u]	8.35[u]
	Dielect.	7.08	5.80	4.33	2.19	4.48	6.10	6.88	6.14	7.36	8.21
	Pseudopot.		1.1	0.6	−0.1	1.4	3.1	3.1	3.0	4.4	
Sn	Expt.			0.3[p]	+0.1[v]	1.6[i]	3.72[i]	3.72[i]	2.40[i]	4.39[i]	4.39[i]
	Dielect.	4.09	0.35	0.18	+0.13	1.48	2.94	2.94	2.41	4.38	4.38
	Pseudopot.		2.0	1.5	0.6	2.1	3.5	3.8	4.1	4.1	
InSb	Expt.	5.07[r]			0.5[p]	2.13[i]	3.27[i]	4.0[p]	4.5[p]	5.25[i]	5.25[i]
	Dielect.	4.61	1.40	1.01	0.39	2.05	3.48	3.77	3.21	4.87	5.07
	Pseudopot.		4.0	3.5	2.0	3.9	5.1	5.6	6.6	7.0	
CdTe	Expt.	6.01[m]			1.80[i]	3.69[i]	5.00[o]	5.9[o]	5.07[o]	6.8[o]	6.8[o]
	Dielect.	6.02	4.32	3.40	1.89	3.73	5.00	5.61	5.03	6.22	6.87
rms	Pseudopot.		0.27		0.24	0.28	0.56	0.61	1.09	0.42	···
dev.	Dielect.	0.22	0.18		0.20	0.21	0.25	0.32	0.37	0.53	0.32

[a] C. D. Clark, P. J. Dean, and P. V. Harris, Proc. Roy. Soc. (London) **A277**, 312 (1964).
[b] R. A. Roberts and W. A. Walker, Phys. Rev. **161**, 730 (1967).
[c] R. J. Archer, R. Y. Loyama, E. E. Loebner, and R. C. Lucas, Phys. Rev. Letters **12**, 538 (1964).
[d] C. C. Wang, M. Cardona, and A. G. Fischer, RCA Rev. **25**, 159 (1964).
[e] W. J. Choyke and L. Patrick, Phys. Rev. **133**, A1163 (1964); **172**, 769 (1968).
[f] B. E. Wheeler, Solid State Commun. **4**, 173 (1966).
[g] F. G. Allen and G. W. Gobeli, Phys. Rev. **144**, 558 (1966).
[h] F. Herman, R. L. Kortum, C. D. Kuglin, and R. A. Short, in *Quantum Theory of Atoms, Molecules, and the Solid State*, edited by P. O. Löwdin (Academic Press Inc., New York, 1966), p. 381.
[i] M. Cardona, K. L. Shaklee, and F. H. Pollak, Phys. Rev. **154**, 696 (1967).
[j] L. R. Saravia and D. Brust, Phys. Rev. **171**, 916 (1968).
[k] P. J. Dean and D. G. Thomas, Phys. Rev. **150**, 690 (1966).
[l] F. Herman, R. L. Kortum, C. D. Kuglin, and J. P. Van Dyke, in *Methods in Computational Physics*, edited by B. Alder, S. Fernbach, and M. Rotenberg (Academic Press Inc., New York, 1968), Vol. 8, p. 193.
[m] R. K. Swank, Phys. Rev. **153, 844** (1967).
[n] R. E. Drews, E. A. Davis, and A. G. Leiga, Phys. Rev. Letters **18**, 1194 (1967).
[o] F. H. Pollak, in *Proceedings of the International Conference on II-VI Semiconducting Compounds, Providence, 1967*, edited by D. G. Thomas (W. A. Benjamin Inc., New York, 1968), p. 552.
[p] M. L. Cohen and T. K. Bergstresser, Phys. Rev. **141**, 789 (1966).
[q] T. E. Fischer, Phys. Rev. **139**, A1228 (1965).
[r] M. L. Cohen and J. C. Phillips, Phys. Rev. **139**, A912 (1965).
[s] Three values of $\Gamma_{25'} \rightarrow \Gamma_{15}$ (referring to the E_0' peak) have been revised from footnote r. These are for GaAs, InAs, and GaSb. In analyzing the photoelectric yield, Cohen and Phillips correctly interpreted the effect of spin-orbit splitting in InSb, but not in the other three cases. The values quoted here place all the crystals on the same footing and are more consistent with the predictions of the present theory, J. C. Phillips (private communication).
[t] T. E. Fischer, Phys. Rev. **142**, 519 (1966).
[u] M. Cardona and G. Harbeke, Phys. Rev. **137**, A1467 (1965).
[v] S. Groves and W. Paul, Phys. Rev. Letters **11**, 194 (1963).

(4) In all cases the absolute value of the $X_4(X_5)$ level, the top of the valence band at the zone edge in the (100) direction, is taken to be a property of the rows of the Periodic Table to which the constituent atoms belong only, i.e., is independent of the degree of ionicity and the actual nearest-neighbor distance. It is determined by extrapolation, in the same manner as the $E_{h,i}$ values, as a function of the normal covalent nearest-neighbor distance.[1] Thus

$$E_{X_4} = (E_{X_4})_{\mathrm{Si}} \left(\frac{(d_A d_B)^{1/2}}{d_{\mathrm{Si}}} \right)^{s_{X_4}} . \qquad (3.3)$$

(5) In all cases, the absolute energy of the $L_{3'}$ (L_{3v}) level, the top of the valence band in the (111) direction, is taken to be the arithmetic mean of the absolute energies of the $\Gamma_{25'}$ (Γ_{15}^{v}) and the X_4 (X_5) levels.

(6) The splitting of the X_1 and X_3 conduction-band states, ΔX, in heterpolar crystals is taken to be a linear function of C only. The absolute energy of the X_1 and X_3 levels are

$$X_1 = X_4 + E_2 - \Delta X \equiv X_4 + E_{2,A} , \qquad (3.4)$$

$$X_3 = X_4 + E_2 + \Delta X \equiv X_4 + E_{2,B} , \qquad (3.5)$$

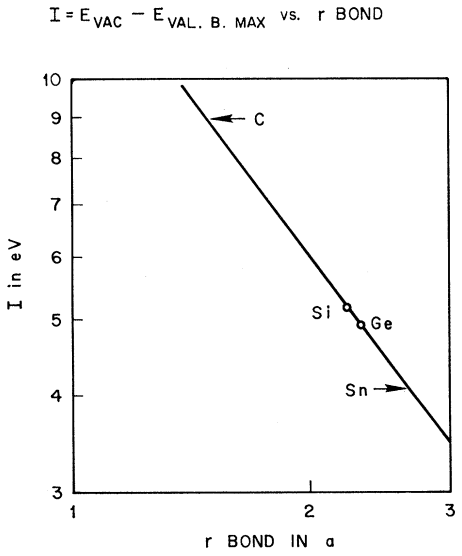

FIG. 1. As are the other homopolar parameters, the ionization potential of the group-IV crystals is assumed to follow a simple power law. Note that unfortunately the two data points, which determine this log-log plot, are very close together.

TABLE IV. Parameters of the 68 compounds considered. In the first column the structure(s) in which the compound is found is indicated using the abbreviation: D for diamond, Zb for zinc-blende, W for wurtzite, and R for the rocksalt or NaCl structure. In the next three columns are found the electronegativity difference (average antisymmetric energy gap) C, the D parameter relating the effective and free-electron plasma frequencies, and the fraction of ionic character on the Phillips scale, f_i. For compounds followed by a †, the values are predicted (see Ref. 1). For purposes of comparison the last two columns contain the f_i values predicted by the theories due to Pauling and Coulson.

Crystal	Type	C (eV)	D	f_i Phillips	f_i Pauling	f_i Coulson *et al.*
C	D	0	1.0	0	0	0
BN	Zb	7.71	1.0	0.256	0.22	0.35
BeO	W	13.9	1.0	0.602	0.63	0.64
LiF	R	23.0	1.0	0.915	0.89	···
BP†	Zb	0.68	1.0	0.006	0.00	0.33
SiC	Zb, W	3.85	1.0	0.177	0.11	0.06
BeS†	Zb	3.99	1.0	0.312	0.22	0.60
AlN	W	7.30	1.0	0.449	0.43	0.36
LiCl	R	11.6	1.0	0.903	0.63	···
MgO	R	14.5	1.0	0.841	0.73	···
NaF	R	20.9	1.0	0.946	0.91	···
Si	D	0	1.0	0	0	0
BAs†	Zb	0.38	1.11	0.002	0.00	···
AlP	Zb	3.14	1.0	0.307	0.01	0.37
MgS	R, W	7.1	1.0	0.786	0.34	···
BeSe†	Zb	3.36	1.08	0.299	0.18	0.60
GaN†	W	7.64	1.11	0.500	0.39	0.36
ZnO	W	9.30	1.08	0.616	0.59	0.65
LiBr	R	9.50	1.03	0.899	0.55	···
NaCl	R	11.8	1.0	0.935	0.67	···
CaO	R	14.6	1.0	0.913	0.79	···
KF	R	16.1	1.0	0.955	0.92	···
CuF†	Zb	15.8	1.06	0.766	0.67	···
BeTe†	Zb	2.05	1.13	0.169	0.09	0.60
AlAs	Zb	2.67	1.11	0.274	0.06	0.37
GaP	Zb	3.30	1.11	0.374	0.06	0.37
ZnS	Zb, W	6.20	1.08	0.623	0.18	0.61
MgSe	R, W	6.41	1.08	0.790	0.29	···
LiI	R	7.40	1.03	0.890	0.43	···
CdO	R	9.15	1.13	0.785	0.55	···
InN†	W	6.76	1.19	0.578	0.34	0.36
CuCl	Zb, W	8.30	1.09	0.746	0.67	0.85
CaS	R	9.10	1.0	0.902	0.43	···
NaBr	R	9.80	1.03	0.934	0.59	···
KCl	R	10.4	1.0	0.953	0.70	···
SrO	R	13.4	1.0	0.926	0.79	···
RbF	R	13.9	1.03	0.960	0.92	···
AgF	R	12.2	1.085	0.894	0.67	···
Ge	D	0	1.26	0	0	0
AlSb	Zb	3.10	1.19	0.426	0.04	0.36
GaAs	Zb	2.90	1.235	0.310	0.04	0.37
InP	Zb	3.34	1.19	0.421	0.04	0.37
MgTe	W	3.58	1.13	0.554	0.18	···
ZnSe	Zb, W	5.60	1.175	0.676	0.15	0.64
CdS	Zb, W	5.90	1.13	0.685	0.18	0.63
CuBr	Zb, W	6.90	1.13	0.735	0.18	0.85
AgCl	R	7.80	1.075	0.856	0.26	···
NaI	R	7.80	1.03	0.927	0.47	···
CaSe	R	8.10	1.0	0.900	0.39	···
SrS	R	8.50	1.0	0.914	0.43	···
KBr	R	9.30	1.025	0.952	0.63	···
RbCl	R	9.70	1.03	0.955	0.70	···
GaSb	Zb	2.10	1.325	0.261	0.02	0.36
InAs	Zb	2.74	1.450	0.357	0.02	0.37
ZnTe	Zb	4.48	1.235	0.546	0.06	0.66
CuI	Zb	5.50	1.175	0.692	0.09	0.84
CdSe	W	5.50	1.235	0.699	0.15	0.61
CaTe	R	6.70	1.125	0.894	0.26	···
AgBr	R	6.90	1.175	0.850	0.18	···
KI	R	7.40	1.025	0.950	0.50	···
SrSe	R	8.00	1.0	0.917	0.39	···
RbBr	R	8.90	1.085	0.957	0.63	···
Sn	D	0	1.46	0	0	0
InSb	Zb	2.10	1.425	0.321	0.01	0.37
CdTe	Zb	4.90	1.303	0.675	0.04	0.61
AgI	Zb, W	5.70	1.213	0.770	0.09	0.84
SrTe	R	6.70	1.10	0.903	0.26	···
RbI	R	7.10	1.075	0.951	0.51	···

where E_2 is given by (3.1) and

$$\Delta X = 0.071C. \tag{3.6}$$

(7) The p-to-s transitions E_0 ($\Gamma_{25'} \rightarrow \Gamma_{2'}$) and E_1 ($L_{3'} \rightarrow L_1$) are affected by the presence of a filled d band in the following way:

$$E_i = (E_{i,h} - (D_{\text{av}} - 1)\Delta E_i)(1 + C^2/E_{i,h}^2)^{1/2}, \tag{3.7}$$

where $i=0$ or 1. As mentioned above and derived in I, D is the square of the ratio of the effective plasma frequency to the free-electron value calculated assuming four electrons per atom (see Table IV). We denote by D_{av} the valence weighted average of the D value of the crystals containing the constituent atoms and the corresponding atom from the same row of the Periodic Table. Thus, e.g., D_{av} of InAs is $\frac{5}{8}$ the D value of InSb and $\frac{3}{8}$ the D value of GaAs. Note that when there is no filled d band, $D = D_{\text{av}} = 1$. Thus (3.7) goes over to (3.1). ΔE_1 and ΔE_0 are parameters which are scaled as a function of nearest-neighbor distance only.

The common feature of (3.1)–(3.8) is that the dependence on C^2 always follows (3.1), i.e., the two-band model. Previous experimental work (e.g., Ref. 17) has been concerned only with horizontal sequences, and has sometimes followed (3.1) and sometimes given $E_{g,i} - E_{h,i}$ proportional to λ^2, i.e., to C^2. We have incorporated this behavior into (3.7) with the aid of the parameters ΔE_i and ΔE_0.

We present in Table III a comparison between our predicted band structure and experiment for 19 tetrahedrally coordinated crystals for which reasonably complete experimental data are available.[18] For purposes of comparison, we include in Table III the predictions obtained from the empirical pseudopotential method as conducted by Cohen, Bergstresser, and Saslow.[4,19,20] We find that while both methods predict values that are generally in very good agreement with

[17] M. Cardona and D. L. Greenaway, Phys. Rev. **125**, 1291 (1962); **131**, 98 (1963).
[18] M. Cardona, K. L. Shaklee, and F. H. Pollak, Phys. Rev. **154**, 696 (1967).
[19] T. K. Bergstresser and M. L. Cohen, Phys. Rev. **164**, 1069 (1967).
[20] W. Saslow, T. K. Bergstresser, and M. L. Cohen, Phys. Rev. Letters **16**, 354 (1966).

experiment, in the cases that our predictions are at variance with the experimental values, they tend to agree with the pseudopotential values. (This may imply inadequate interpretation of broad-band optical data. The values shown were estimated by the experimentalist who took the data and may be revised in the future.)

Two discrepancies do merit comment. In GaP, AlSb, and GaAs it is believed that the lowest indirect gap is from Γ to X (or Δ). This designation is made on the basis of the observation that this gap in these materials decreases with hydrostatic pressure.[21] The Γ-to-X indirect gap in Ge, which is not the lowest indirect gap in Ge, is also observed to decrease with pressure,[21] whereas all other gaps, direct and indirect, increase with pressure. Thus one concludes that the smallest indirect gap in GaP, AlSb, and GaAs must also be from Γ to X.

However, we see in Table III that our simple calculation has predicted that the smallest indirect gap in GaP and GaAs is from Γ to L, as it is in Ge. We note that the predicted magnitude of the gap in GaAs agrees very well with the experimental value. In GaP the predicted magnitude of the gap is 0.37 eV larger than experiment, but the predicted E_1 gap ($L_{3,v} \rightarrow L_{1,c}$) is also 0.16 eV too large so that if E_1, which by (3.7) is strongly dependent on the D values which we do not know with accuracy,[1] were correct, then the discrepancy would be 0.21 eV. In I we observed that AlSb was one of the most atypical of the zinc-blende crystals. In Table III we see that we have predicted that the lowest indirect gap is to X, but the predicted magnitude is 0.29 eV too large. However, one of the worst errors in the entire survey occurs in our prediction of the E_1 gap in AlSb. The predicted value is 0.49 eV too large. Moreover, if E_1 were correct, then the magnitude of the indirect gap would be 1.87 eV, which is in exact agreement with experiment, but the direction would again be Γ to L.

The empirical pseudopotential method encounters the same problem in accounting for a reversal of the X and L levels in the conduction band on going from Ge to GaAs, GaP, and AlSb. In their calculation, Cohen and Bergstresser[4] elected to fix their antisymmetric local pseudopotential form factors in order to obtain reasonable agreement with the Γ-to-X indirect gaps at the expense of errors of 1.0, 0.7, and 0.4 eV, respectively, in the direct, X_5-X_1, E_2 gap. Even so, Cohen and Bergstresser still predict that the Γ-to-L gap in GaAs would be lower than Γ to X and in AlSb the two would have the same value.

We must conclude that if the above argument about the pressure dependence of the gap is correct, then neither the local empirical pseudopotential nor our simple two-band method can account for the level reversal. Because our method nowhere involves any consideration of the crystal-structure factors, perhaps we should not be surprised that it does not predict this change in geometry and instead be content that we have reasonable agreement in the magnitudes of both the direct and the indirect gaps. We also note that for GaSb, where the local pseudopotential again has severe trouble with the indirect gaps (although our method gives good results), Zhang and Callaway[22] have shown that a nonlocal pseudopotential can give good results for the band structure and also for its pressure dependence. Unfortunately, their nonlocal calculation for one crystal requires 14 empirically determined parameters.[22]

The second discrepancy that we note in Table III is that our method predicts the $E_{1'}$ gap well enough for the homopolar cases but does not show it increasing with electronegativity difference C rapidly enough. Thus we conclude that the p-like $E_{1'}$ transition is more sensitive to the antisymmetric potential than is the band structure as a whole. To correct for this, we have recalculated the $E_{1'}$ gaps with C increased by 20%. We list these values in the last column in Table III, where we see that agreement with experiment is substantially improved.

IV. UNIVERSAL SEMICONDUCTOR MODEL

At this point we insert a qualitative discussion of the concept and motivation underlying the relations just presented. All of these relations conform to a dielectric two-band model. While other relations have been tried (such as a linear dependence of E_g on C^2), it has been found that (1.1) does indeed give best results.

Where the initial assumptions need modifying, as occurred in the case of the C dependence of $E_{1'}$, we do so, but our primary purpose is to show how much can be done without elaborate calculation. It might be said that we are trying to develop a semiconductor analog to the valence-bond theory.[23] We call this the universal semiconductor model. As we have already noted, it is a two-band model. This corresponds to the chemist's notion of bonding and antibonding states and the reason that our model is so successful may well lie in the basic validity of this chemical notion.[23]

Consider first the valence band. We limit our description to the specification the energy of the band at the three principle symmetry points Γ, X, and L. (As noted in Table I, critical points in the real crystal sometimes lie small distances away from these points, but we do not attempt to account for this geometric detail.) These three energies are specified by assumptions (3)–(5) of Sec. III. Recall that bands are formed in an elemental crystal because of the interaction of the free atomic wave functions as the atoms are brought close together. The closer together the atoms come, the more

[21] R. Zallen and W. Paul, Phys. Rev. **155**, 703 (1967).

[22] H. I. Zhang and J. Callaway, Solid State Commun. **6**, 515 (1968); Phys. Rev. **181**, 1163 (1969).

[23] C. A. Coulson, L. R. Redei, and D. Stocker, Proc. Roy. Soc. (London) **A270**, 357 (1962).

the spread of the atomic levels, i.e., the wider the bands. Because this is a band spreading effect, we would expect some state in the valence band to be degenerate with the highest level of the ground-state configuration of the free atom. Now in a heteropolar crystal, i.e., when $C\neq 0$, the effect of increasing C, and thus ionicity, is to decrease the width of the bands until finally the electronic states become well localized into an ionic configuration and the bands are flat, as when the neutral atoms were separated. Again we might expect that some state in the valence band is going to remain constant as the width of the band is reduced. These speculations have been crystalized in assumption (4), where we take X_4 (X_5) to be the level that is independent of C. Although, as with all energy parameters, we scale the X_4 energy level with distance, we note that the values assumed for Si and Ge, which determine the extrapolation, -8.63 and -8.14 eV, respectively, are within 5% of the free-atom ionization potentials, 8.15 and 7.88 eV. (The extrapolated values for C and Sn are 15.74 and 6.69 eV, compared with free-atom ionization potentials of 11.26 and 7.33 eV.) We used the normal covalent nearest-neighbor distance in assumption (4) instead of the observed value, because, as just stated, we are assuming that the X_4 (X_5) level will stay constant independent of the effects of the antisymmetric potential C, which are the cause of the deviations from the normal covalent valent value. This distinction makes little difference for the 19 crystals in Table III (e.g., it would improve the value of the indirect gap in GaP by 0.1 eV), but it makes a big difference when we go to the NaCl structure. There the ionization potential would be 1 eV or more too low if d were used in (3.3).

Having fixed the valence level at X, we consider the problem of specifying the width of the band. Perhaps the first approach to come to mind would be to specify a homopolar width that would be a function of nearest-neighbor distance only and then specify how the actual width is related to this homopolar value and C. We have instead made assumption (3), i.e., used Eq. (2.1), because such a project would require at least twice as many parameters which would have to be determined from a combined analysis of the I, E_2, and indirect gaps of not only the group-IV elements but also several heteropolar crystals. Because we test the validity of our model by trying to predict the energy gaps of as many crystals as possible, we wish to restrict ourselves to the group-IV crystals when fixing parameters whenever possible. In the present formulation only the magnitude of the X_1, X_3 splitting is determined by the heteropolar crystals. The alternative prescription for the band width could have the advantage that in the limit of large C, we would not have the Γ level dropping far below the X level thus giving a large (negative) band width. It is well known from band calculations that this does not happen. The level at Γ is only slightly below that at X (or L) in NaCl-type and some wurtzite-type crystals. However, we see in Sec. V that in our formulation this catastrophe is avoided by a change in crystal structure. In effect, we propose that the crystal structure changes to prevent such an occurrence.

We complete the specification of the valence band by fixing the L level. It seems clear to us that the simplest prescription is that the L level is intermediate between Γ and X, i.e., assumption (5).

Having specified the valence band, the conduction band is determined by the interband energy gaps. Assumption (1) says that in the absence of d-state perturbation all gaps vary with C as does the average gap E_g. In assumption (2) we take all homopolar parameters to be simple power-law functions of nearest-neighbor distance only.

The d-state perturbation is formulated in assumption (7). It was arrived at as follows. First the homopolar part of E_0 and E_1 gaps was determined by the experimental value in Si, the author's estimate of the experimental value in C, and the power-law assumption. Then the amount by which the conduction-band s states were lowered due to the d states in the ion cores could be determined for the pure homopolar case by observation of the levels in Ge and Sn. This homopolar effect was separated into two factors. One factor, the ΔE_i, is taken to be a function of nearest-neighbor distance only. The other factor is taken to be proportional to the oscillator strength connecting the d band and the valence band,[1] i.e., the $D-1$ factor. When we go from the homopolar to the heteropolar crystals, we assume that both the unperturbed homopolar gap and the perturbation are increased by the same square-root factor.

Now we come to the fact that the valence weighted average D value D_{av} is used in (3.7) instead of the D factor for the band as a whole as found in I. First we note that there is no distinction between the two values, i.e., $D=D_{\text{av}}$ for the homopolar crystals and for those heteropolar crystals for which both elements are from the same row. The only distinction is in the skew compounds. Considering a pair of skew compounds such as GaSb and InAs or AlSb and InP, we see that the D values of the two members are the same[1] but the D_{av} values are quite different. We have used D_{av} in (3.7) rather than D because we observe that the E_0 and E_1 gaps in InAs and InP are substantially smaller than in GaSb and AlSb. If D were used the reverse would be predicted. It may be that the reason for this is that the effect occurs in the core region, where the effect of the other atom is negligible. Thus the effect of the In core on an s electron in InAs is better given by the total band d effect found for InSb than that in InAs. However, we note that when one of the skew elements belongs to the first row, this *ad hoc* prescription does not work very well. For the case of InN, it would predict that the Γ_1 level would lie 0.1 eV below the Γ_{15}

level and the compound would be a metal. On the other hand, if we use D instead of D_{av} we get a very reasonable result. (See Table VII.) It must be admitted that this point is still unresolved.

Despite the above difficulty, we have been able to retain the minimum possible number of assumptions to formulate a model band structure that agrees with experiment better than other empirical methods which use several times as many parameters.

V. CRYSTAL STRUCTURES

In Fig. 2 we have plotted the values of our parameters E_h and C, the homopolar and heteropolar energy gaps for the 59 crystals for which we were able to establish an experimental value for C in I. We distinguish these according to the crystal structure in which the compound is found. The C-versus-E_h plot is seen to separate into three regions. All compounds which form NaCl-type crystals are found in the most ionic region, A, while all compounds which form only zinc-blende-type crystals are found in the most covalent region, D. In the narrow intermediate region, B, compounds are found in the wurtzite structure. In the low E_h region, which is included in the insert, several compounds near the boundaries between regions are found in both structures. As E_h increases, a wide gulf in which no compounds are found opens between the NaCl and the wurtzite regions.

We propose that the curves shown in the figure are the boundaries between regions. They are calculated as described below.

The boundary between the zinc-blende and wurtzite regions is the curve for which we would calculate

$$I=E_{X_5}, \tag{5.1}$$

where, as described in Sec. III, the absolute energy of the top of the valence band at X, E_{X_5} is calculated using (3.2) as a function of the normal covalent nearest-neighbor distance only, and the top of the valence band at Γ, I is calculated as a function of nearest-neighbor distance and C using (2.1).

The curve shown in Fig. 2 between regions A and B is that for which $f_i=0.785$. Here f_i is the fraction of ionic character,[1,3] defined as

$$f_i=C^2/(E_h^2+C^2). \tag{5.2}$$

In Table IV we see that MgSe and MgS, which are metastable in the wurtzite structure,[24] have f_i values which are slightly higher than this value.

However, we note that another boundary may also be proposed on the assumption that the valence band at Γ, as predicted by (2.1), may only be a certain amount $\Delta E(d)$ below the level at the zone boundary, E_{X_5}, as predicted by (3.3). If we assume

$$\Delta E(d)=1.5(d_{Si}/d)^2 \text{ eV}, \tag{5.3}$$

[24] H. Mittendorf, Z. Physik **183**, 113 (1965).

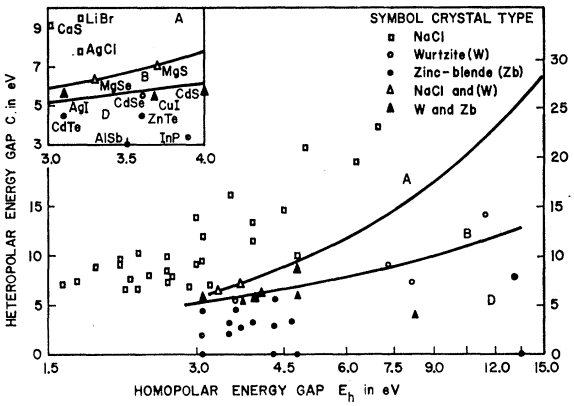

FIG. 2. Crystal-type distribution in E_h-C plane. The boundary shown between regions B and D is where we calculate the top of the valence bond at Γ to be degenerate with that at X. The boundary shown between regions A and B is where $f_i=0.785$.

then this boundary would lie close to, but lower than, the $f_i=0.785$ boundary in the insert region, and much lower in the large E_h region on the right half of the figure. This alternative boundary would pass slightly above BeO and no compound found stable in the wurtzite structure would lie above it. We suggest that the reason for the gulf between the wurtzite and NaCl crystals may be that a wurtzite-type crystal can not tolerate having its valence band at the zone center substantially lower than at the zone boundary and that the NaCl structure is not stable unless the compound is sufficiently ionic.

As the notion that crystal structure is dependent on degree of ionicity is not at all new,[25] we compare in Table IV the values of f_i on the Phillips scale (5.2) with the values proposed by Pauling[26] and by Coulson *et al.*[23] It has been noted[25] that if one were to use the Pauling scale of ionicity and assume that there is some critical value of f_i such that if a compound has a value greater than this critical ionicity it must form an octahedral crystal such as rocksalt, and if less a tetrahedral structure, then one could not make fewer than eight errors among the 68 crystals in Table IV. (See Fig. 3.) If one were to take as the critical value either that of MgS or of MgSe, which clearly must be borderline cases because they are found with both coordinations, then, using the Pauling scale, one would make substantially more than eight errors. However, with the Phillips scale one may use either criterion and make no errors at all in predicting the coordination of the crystal structure assumed. It may be fair to point out that one could naively propose, merely by glancing at the Periodic Table, that all alkali halides and all alkaline earths are to be found in the NaCl structure and everything else is to be found

[25] J. C. Phillips, *Covalent Bonding in Crystals, Molecules and Polymers* (The University of Chicago Press, Chicago, to be published).

[26] L. Pauling, *The Nature of the Chemical Bond* (Cornell University Press, Ithaca, N. Y., 1960), pp. 91 ff.

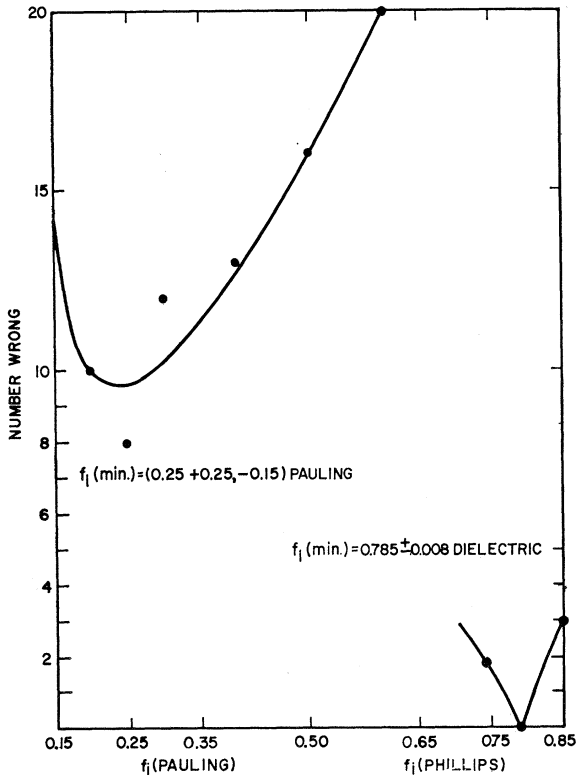

FIG. 3. Comparison of the Pauling and Phillips ionicity scales in ability to predict coordination number of binary compounds. While the minimum possible number of errors using the Pauling scale is 8, no errors are made using the Phillips scale if the critical value of f_i is chosen to be 0.785.

in a tetrahedral structure. With such a criterion, one would make nine errors—only one more than the minimum possible using Pauling's scale.

Coulson *et al.*[23] do not apply their valence-bond ionicity scale to any but tetrahedrally coordinated crystals because their theory is restricted to (sp^3)-type bonding. (We showed in I that the dielectric theory, and thus the Phillips scale, can be extended at least to the NaCl-type crystals without difficulty.) The ionicity values of Coulson *et al.* are included in Table IV for purposes of comparison. One can see that Coulson's values range from 0 to 85%, but that the compounds that they would call most ionic, i.e., CuCl, CuBr, CuI, and AgI, are found in both zinc-blende and wurtzite structures, while AlN, GaN, and InN, which occur only in wurtzite, are less than half as ionic on their scale. We conclude that the Coulson scale is not substantially superior to the Pauling scale.

In another respect also the Phillips ionicity scale is useful in predicting crystal structures. It is well known[27] that under pressure the group-IV elements and the more covalent of the III-V compounds undergo a phase transformation to the β-tin structure in which they are metallic at ordinary temperatures and superconducting at low temperatures. More ionic crystals undergo a phase transformation to the NaCl or to the cinnabar structure in which they are insulators at all temperatures. We discuss this in detail elsewhere,[9] but here we note that the dividing point between these two possibilities falls at about 32% ionic character.

We will now try to understand the transition from zinc-blende to wurtzite structure with increasing electronegativity difference. In Fig. 4 we note that the difference between these two tetrahedrally coordinated structures lies in the relative positions of the third nearest neighbors. Take the example of ZnS and consider one Zn-S bond. The situation is analogous to that of ethane (C_2H_6), where the C-C bond corresponds to our Zn-S bond. Just as each C is tetrahedrally bonded to three hydrogens, so in ZnS each of our atoms is bonded to three other opposite atoms. Ethane may exist in two states, which are referred to as eclipsed and staggered. (See Fig. 4.) The staggered state is obtained from the eclipsed state by rotating one of the H triads $\frac{1}{3}\pi$ about the C-C axis. The wurtzite structure corresponds to the eclipsed conformation if one identifies the C-C axis of the ethane with the c axis of that hexagonal structure. The zinc-blende structure corresponds to the staggered state where the C-C axis corresponds to the (111) body diagonal of the cube.

It appears from Fig. 4 that the Coulomb attraction of the third-nearest-neighboring Zn and S atoms (which are partially ionized) favors the wurtzite structure. However, the Madelung constant for the ideal wurtzite structure is only 1.639,[28] as compared to 1.638 for zinc blende. Thus the difference in Coulomb energy is negligible.

In ethane the staggered state has the lower energy. It might be thought that this is due to Coulomb repulsion of the partially charged H atoms. Actually,

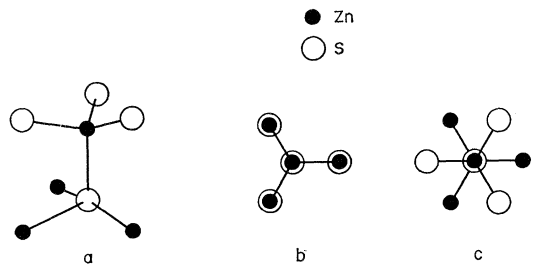

FIG. 4. Comparison of the two tetrahedrally coordinated structures, zinc-blende and wurtzite, for the case of ZnS: (a) is a perspective view for either structure; (b) the wurtzite structure, which is analogous to the eclipsed configuration in ethane, as seen looking down the c axis; (c) the zinc-blende structure,which is analogous to the staggered configuration in ethane, as seen looking down the [111] body diagonal.

[27] See W. Klement, Jr., and A. Jayaraman, in *Progress in Solid State Chemistry*, edited by H. Reiss (Pergamon Publications Corp., New York, 1966), Vol. 3, p. 289; also A. Jayaraman, W. Klement, Jr., and G. C. Kennedy, Phys. Rev. **130**, 540 (1963); **130**, 2277 (1963).

[28] M. Born and K. Huang, *Dynamical Theory of Crystal Lattices* (Oxford University Press, London, 1966), p. 155.

TABLE V. Energy levels of ZnS and of a hypothetical compound having the same parameters as ZnS except the antisymmetric potential, which is taken to be zero, calculated by the pseudopotential method for the zinc-blende, wurtzite, and rocksalt (NaCl) structures. The zinc-blende and wurtzite calculations were performed by Dr. T. K. Bergstresser (see Ref. 19). The values quoted for the wurtzite structure are those corresponding to the Γ and L points in the zinc-blende Brillouin zone (see Ref. 19).

	$V_a=0$						$V_a\neq 0$					
		Γ			L			Γ			L	
Level	Zb	W	R	Zb	W	R	Zb	W	R	Zb	W	R
1	0	0	0	3.27	3.32	3.47	0	0	0	0.90	0.89	0.85
2	17.41	17.44	12.28	7.32	7.22	3.47	19.81	19.88	16.31	14.59	14.57	12.60
3	17.41	18.18	12.66	15.78	15.82	13.61	19.81	19.88	16.31	19.12	19.05	15.95
4	17.41	18.18	12.66	15.78	15.87	13.61	19.81	19.88	16.31	19.12	19.05	15.95
5	21.33	21.59	12.66	19.46	19.46	13.61	24.80	24.84	19.74	26.79	26.98	21.91
6	22.10	21.59	18.77	22.95	25.05	13.61	31.06	31.07	26.68	31.14	32.84	24.36
7	22.40	21.85	18.77	22.95	25.05	15.85	31.06	31.07	26.68	31.14	32.84	24.38
8	22.40	23.21	18.77	28.38	26.53	15.65	31.06	31.47	26.68	···	34.17	29.51

this effect accounts for only a very small fraction of the energy difference. Molecular-orbital calculations[29] have shown that most of the repulsion arises because the electron wave functions between the cis H atoms in the eclipsed configuration are antibonding. Put simply, the kinetic energy of the valence electrons is greater when they are confined to a two-dimensional cis channel in the eclipsed configuration than when they are delocalized in three dimensions.

In crystals also the kinetic energy favors the staggered zinc-blende structure. Thus the group-IV elements and the more covalent heteropolar compounds are found in this structure. In order to make this observation somewhat more quantitative, we consider the results of a pseudopotential calculation. In Table V we present the energy levels at Γ and at L calculated by Bergstresser and Cohen[19] for ZnS and for a hypothetical crystal having the same parameters as ZnS except that the antisymmetric potential has been set equal to zero. To complete the comparison of crystal structures, we have calculated the energy levels for two more hypothetical crystals having the NaCl structure, the same density, and the corresponding pseudopotential form factors.

Consider first the $V_a=0$, i.e., homopolar, situation. It is immediately apparent from Table V that in the NaCl structure the substance would be a metal. Because metallic binding is much weaker than covalent or ionic binding, homopolar compounds do not form crystals with the NaCl structure. Comparing zinc blende and wurtzite, we see that the average of the top three valence bands at Γ in wurtzite is 0.52 eV higher than the threefold $\Gamma_{25'}$ level in zinc blende. (Contrary to the normal convention, which is to measure energy relative to the valence-band maximum, we have measured it relative to the lowest valence band, Γ_1, because this level is least sensitive to changes in third-nearest-neighbor interactions and thus makes comparisons of the other levels meaningful. Of course, when we change the nearest-neighbor distance by going to the NaCl structure, we expect all levels to be affected significantly.) Clearly, raising the energy of the valence-band levels will lower the cohesive energy of the crystal. This effect falls off as one goes toward the zone boundary, so that the average effect is much less than 0.5 eV per valence electron.

Now let us consider the situation with the antisymmetric potential turned on. We see that in the NaCl structure, ZnS would be a semiconductor but with substantially smaller gaps. Because the single-particle energy decreases monotonically with increasing average energy gap,[30] the NaCl structure is not favored at normal pressures for which a larger average gap may be had in a tetrahedral structure. Comparing zinc blende and wurtzite we see that, as originally noted by Bergstresser and Cohen,[19] in ZnS the corresponding energy levels are virtually identical in the two structures. Indeed the reflectivity spectra of the two crystals have been observed to be virtually identical.[31] (See Fig. 5, which has been borrowed from Cardona and Harbeke.[31]) Thus the differences in the antisymmetric structure factors between zinc blende and wurtzite favor the wurtzite and compensate for the effects of the symmetric potential which favor zinc blende.

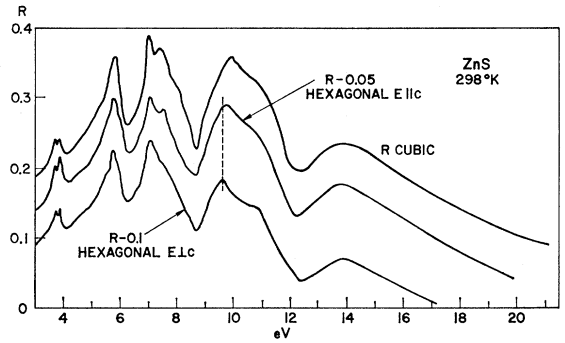

FIG. 5. Reflection spectra of room-temperature ZnS in zinc-blende (cubic) and wurtzite (hexagonal) structures reported by Cardona and Harbeke (Ref. 31).

[29] J. A. Pople and G. A. Segal, J. Chem. Phys. **43**, 5136 (1965).

[30] J. A. Van Vechten, Phys. Rev. **170**, 773 (1968).

[31] M. Cardona and G. Harbeke, Phys. Rev. **137**, A1467 (1965).

VI. EXTENSION TO NaCl STRUCTURE

In this section we probe the limits of applicability of our two-band dielectric model. We try to predict the direct band gap of compounds in the NaCl structure. We use the simplest reasonable theory, make no empirical corrections, and defer the calculation of the entire band structure to a later paper.

Unlike wurtzite, the NaCl structure differs from the zinc-blende structure in the arrangement of nearest neighbors. Although our dielectric definition ensures that our average E_g must correspond fairly well with the largest peak in the absorption spectrum, the observation made in Sec. V that a homopolar crystal in the NaCl structure would be a metal indicates that we can not take account of the change in the nearest-neighbor interaction merely by taking account of the increased nearest-neighbor distance via Eq. (3.2). The difference in the structure factors between the diamond and NaCl structures causes a reordering of some of the valence- and conduction-band levels for a homopolar compound.

Equations (3.1) and (3.2) cannot yield such level reversals. They allow only for a change in valence to conduction-band gap with changing d and C.

We believe that the logical way to treat this effect of the change in the structure factors is to calculate the band structure of a hypothetical homopolar compound in the NaCl structure using the pseudopotential method. This has been done for the case of Si (see Fig. 6). From the form factors found by Cohen and Bergstresser[4] for diamond-type Si, we deduce the corresponding form factors for an NaCl-type crystal of the same density. The values we have used are $V^s(200)=-0.15$, $V^2(220)=0.04$, and $V^s(222)=0.08$ Ry. The calculated band structure is shown in Fig. 6. The largest calculated negative direct gap, i.e., the largest energy difference between states that in the actual crystal would form the valence and conduction bands and for which the state corresponding to the conduction band lies below the state corresponding to the valence band, is 7.7 eV. (This occurs at the point K.) As with the zinc-blende crystals, the phase difference between the symmetric and antisymmetric potentials in the unit cell implies that we must combine the squares of E_h and of C to obtain the square of E_g. However, we must also take account of the level reversals where they occur. Thus for those cases in which the homopolar potential acts to reverse the order of the levels from what it is in the predominately ionic actual crystal, we assume, instead of (3.1),

$$E_{g,i}^2=C^2-E_{h,i}^2. \tag{6.1}$$

Because we lack any sort of empirical determination of the dependence of the negative homopolar gaps, we will assume that they vary approximately as the average homopolar gap was found to vary in I. Thus we assume

$$E_{b,h}=7.7(a_{\mathrm{Si}}/a)^{2.5}\ \mathrm{eV}, \tag{6.2}$$

where a is the crystal lattice constant and $E_{b,h}$ is the homopolar value of the (lowest) direct band gap.

The calculation outlined above has been performed, and the results are presented in Table VI. The band structures of NaCl-type crystals are not nearly as well investigated as are those of the semiconductors treated in Sec. III. Therefore, we have shown as many estimates of the direct band edge as we are aware of in the experimental data.

While the agreement of this crude theory with experiment is not nearly as good as was found with the semiconductors, it is fair for the alkali halides which do not contain a first row element. For the least ionic of the NaCl-type crystals, MgS, MgSe, and CdO, the above calculation yields a negative gap. The value shown in Table VI with the dagger is that calculated for the same compound in the wurtzite structure. Because MgS and MgSe are metastable and CdO should be almost stable in the wurtzite structure, these values seem to be approximately correct for the stable crystal.

It is to be hoped that when more experimental data become available, it will be possible to refine this crude theory considerably.

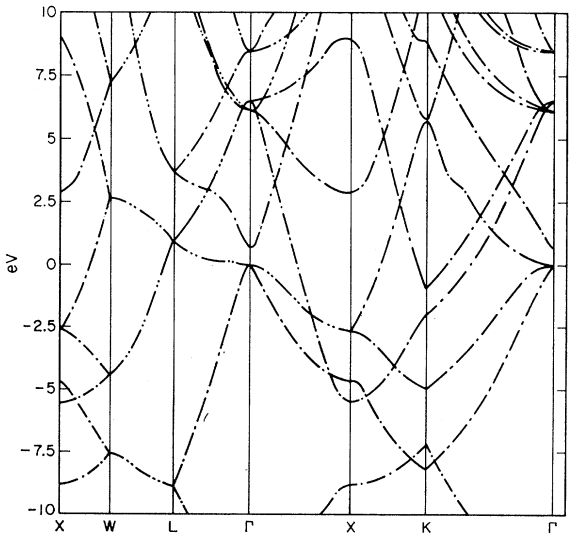

FIG. 6. Calculated band structure of a hypothetical crystal having the density and pseudopotential of Si but the NaCl structure.

VII. CONCLUSIONS

We have presented a method of predicting interband energies which is based on a generalization of the usual two-band model (bonding and antibonding sp^3 orbitals) to treat arbitrary diatomic combinations containing eight valence electrons per unit cell. In our two-band model, a direct connection is established between the *average* energy gap E_g and the electronegativity difference between the constituent elements, C. The inter-

TABLE VI. Lowest direct band gap of 28 NaCl-type crystals using no adjustable parameters (see text). For compounds followed by a dagger, the values were calculated for the wurtzite structure and it is postulated the same value should obtain in the NaCl structure.

Crystal	Band gap (calc., eV)	Band gap (expt.)
LiF	16.2	13.6[a]
LiCl	7.5	9.3[b]
LiBr	5.8	7.95[c]
LiI	4.3	
NaF	17.4	
NaCl	9.4	8.6,[b] 9.0,[d]
NaBr	7.5	7.6,[b] 7.5[c]
NaI	5.9	5.8,[b] 6.75[c]
MgO	4.0	7.8[d]
MgS†	7.7	
MgSe†	6.3	6.0[e]
KF	14.0	
KCl	8.9	8.9,[f] 8.5,[b] 8.5,[c] 8.7[d]
KBr	7.9	8.0,[f] 7.7,[b] 7.2[c]
KI	.6.2	6.3,[f] 6.1,[b] 6.1[c]
CaO	10.2	9.8[g]
CaS	6.0	
CaSe	4.9	
CaTe	3.9	
RbF	11.7	
RbCl	8.3	8.5,[f] 8.2[b]
RbBr	7.5	7.5,[b] 7.65[c]
RbI	5.9	6.3,[f] 6.0,[b] 6.0[c]
SrO	10.2	
SrS	6.1	
SrSe	5.8	
SrTe	4.3	
CdO†	2.5	2.4[h]

[a] D. M. Roessler and W. C. Walker, J. Phys. Chem. Solids **28**, 1507 (1967).
[b] Assignment made by the author on the basis of spectra reported by Teegarden and Baldini (footnote f).
[c] J. C. Phillips, Phys. Rev. **136**, A1705 (1964).
[d] D. M. Roessler and W. C. Walker, Phys. Rev. **166**, 599 (1968).
[e] H. Mittendorf, Z. Physik **183**, 113 (1968).
[f] K. Teegarden and G. Baldini, Phys. Rev. **155**, 896 (1967); assignment made by Teegarden and Baldini.
[g] R. C. Whited, thesis, University of California, Santa Barbara, 1969 (unpublished); R. C. Whited and W. C. Walker, Phys. Rev. Letters **22**, 1428 (1969). Assignment made by author.
[h] M. Altwein, H. Finkenrath, C. Konak, J. Stuke, and G. Zimmer, Phys. Status Solidi **29**, 203 (1968).

band energies are then predicted from C and observation of the previously determined interband energies in Si. The effect of core d states in third- and fourth-row elements is added as a perturbation.

Previously, attempts have been made[32] to establish direct relations between individual interband energies and the valence difference λ, which is approximately proportional to C. In particular, linear relations between the lowest direct gap, usually E_0, and λ have been proposed.[32] We believe that our method—of concentrating first on the average gap and the dielectric constant and then treating individual interband energies after C has been determined independently—provides a considerably more coherent and meaningful analysis. Our method uses many fewer parameters, explains the slopes and curvatures of the λ^2 plots, explains the trends from one sequence to the next, and provides a useful generalization of the valence difference parameter λ. Although most previous workers concentrated on E_0, we believe that this was a particularly bad choice because of the sensitivity of the Γ_1 level to the effects of core d states as shown by (3.7) and the magnitude of the ΔE_0 parameter in Table II. Rather than postulating a linear λ dependence for E_0, as opposed to the parabolic dependence predicted by Herman's[6] original model, we have predicted the observed E_0 values for heteropolar crystals from observation of the dielectric constants and the E_0 values in the purely homopolar crystals, Ge and Sn.

An attractive feature of our model is the small number of parameters required to describe a large number of interband transitions. Altogether we have 19 adjustable parameters and have obtained good results for 19 tetrahedrally coordinated crystals. Thus we have one adjustable parameter per crystal as compared to an average of three per crystal for either the (local) empirical pseudopotential method[4,19,20] or the empirically refined orthogonalized-plane-wave method developed by Herman and co-workers.[33,34] Other methods (such as the nonlocal pseudopotential,[21] the tight-binding method,[35] and the extended $\mathbf{k}\cdot\mathbf{p}$ method[36,37]) require an order of magnitude more parameters. Moreover, all our parameters except the X_1–X_3 splitting are determined by the four homopolar crystals, so that we might claim that we have fitted the band structures of 15 crystals without any free parameters.

The last feature allows us to predict the band structures of heteropolar crystals from a knowledge of the dielectric constant and the lattice constant alone. When an experimental value for the dielectric constant is not available, we may use the value predicted in I, but the result should be considered somewhat more tentative. We also expect to have more difficulty with compounds containing one first-row and one non-first-row element, because of the nonlocal antisymmetric contribution to the pseudopotential arising from the lack of core p states in first-row elements. With these qualifications, we present in Table VII our predictions for the 18 tetrahedrally coordinated crystals for which little experimental evidence is available, and which were not included in Table III. However, our method is limited to high symmetry points and thus cannot replace pseudopotential and other methods for the purpose of calculating $\epsilon_2(\omega)$ spectra, etc.

We have also presented what is to our knowledge the first general discussion of the ionization potentials of tetrahedrally coordinated crystals.

[32] Cf. M. Cardona and D. L. Greenaway, Phys. Rev. **131**, 98 (1963).

[33] F. Herman, R. L. Kartum, C. D. Kuglin, J. P. Van Dyke, and S. Skillman, in *Methods in Computational Physics*, edited by B. Alder, S. Fernbach, and M. Rotenberg (Academic Press Inc., New York, 1968), Vol. 8, p. 193.
[34] D. J. Stukel, R. N. Eunema, T. C. Collins, F. Herman, and R. L. Kortum, Phys. Rev. **179**, 740 (1969).
[35] J. C. Slater and G. F. Koster, Phys. Rev. **94**, 1498 (1954).
[36] E. O. Kane, J. Phys. Chem. Solids **1**, 82 (1957); **1**, 249 (1957).
[37] M. Cardona and F. H. Pollak, Phys. Rev. **142**, 530 (1966).

TABLE VII. Predicted values of ionization potential and interband energy gaps in eV for the tetrahedrally coordinated compounds not included in Table III. Experimental data are not conclusive for these crystals and predictions are tentative, particularly for the oxides. Spin-orbit splitting is neglected. For those compounds followed by a dagger, the value of $\epsilon(0)$ and thus C used are those predicted in Ref. 1. The calculation is the same as that in Table III except, as noted in Sec. IV, D is used instead of D_{av} in Eq. (3.7).

Crystal	I	Indirect gaps Γ to X	Γ to L	E_0	E_1	Direct gaps E_{2A}	E_{2B}	E_0'	E_1'
BN	11.70	9.57	9.75	14.74	11.77	13.60	14.70	10.71	14.87
BeO	15.74	16.42	···	17.65	15.99	16.42	18.34	15.43	19.79
AlP†	6.03	2.63	3.45	5.13	4.75	5.23	5.68	4.61	6.97
CuBr	8.14	7.45	6.43	4.99	6.43	7.45	8.43	7.54	9.87
AgI	6.69	6.02	5.07	3.47	5.20	6.02	6.83	6.20	8.13
BeS†	7.20	2.38	3.89	6.88	6.11	6.84	7.40	5.81	8.59
AlN	10.02	8.35	···	10.43	9.34	9.99	11.02	8.94	12.19
GaN†	10.12	6.39	···	4.80	7.00	9.87	10.96	9.08	12.24
ZnO	11.32	8.94	···	7.25	8.94	11.01	12.36	10.62	13.86
CuF†	11.32	16.62	14.68	12.85	14.68	16.62	18.86	16.72	20.94
BAs†	6.13	0.91	1.17	3.14	3.76	6.10	6.15	4.37	7.33
BeSe†	6.58	1.30	2.29	4.23	4.66	6.04	6.52	5.13	7.75
InN†	8.91	4.70	···	3.22	5.36	8.27	9.23	7.87	10.61
BeTe†	5.44	−0.18	0.93	2.69	3.33	4.61	4.90	3.86	6.21
AlAs	5.63	2.00	2.32	3.14	3.69	4.75	5.14	4.17	6.44
CuCl	8.38	8.88	8.43	7.82	8.43	8.88	10.05	8.98	10.21
MgTe†	5.51	2.38	2.83	3.21	3.88	4.46	4.97	4.38	5.76
CuI	7.11	5.85	4.94	3.61	5.07	6.12	6.91	6.16	8.24

We have suggested how crystalline structures may be predicted on the basis of predicted band structures. In our opinion this approach is considerably more promising that the traditional attempt to calculate total cohesive energies in the various possible structures to determine in which one the compound will be found. The energy differences between various structures is so small as to be beyond the limits of accuracy of any cohesive energy calculation in the foreseeable future.

We have predicted the band gap of 28 compounds in the NaCl structure using no empirically adjusted parameters at all. While the results are not as satisfactory as those for the tetrahedrally coordinated crystals, they allow one to hope that the method could be satisfactorily extended to octahedrally coordinated systems if sufficient empirical information were available.

ACKNOWLEDGMENTS

The author is deeply grateful to James C. Phillips for his continuous guidance and inspiration and to Dr. T. K. Bergstresser for many helpful discussions and comments and especially for permission to use some of his unpublished data in Table V. He is also grateful to Professor Manuel Cardona for permission to reproduce Fig. 5.